

Ab initio calculations of structures and stabilities of $(\text{NaI})_n\text{Na}^+$ and $(\text{CsI})_n\text{Cs}^+$ cluster ions

Andrés Aguado

Departamento de Física Teórica, Facultad de Ciencias, Universidad de Valladolid, 47011 Valladolid, Spain

Andrés Ayuela

Laboratory of Physics, Helsinki University of Technology, 02015 Espoo, Finland

José M. López and Julio A. Alonso

Departamento de Física Teórica, Facultad de Ciencias, Universidad de Valladolid, 47011 Valladolid, Spain

(Received 12 February 1998)

Ab initio calculations using the perturbed ion model, with correlation contributions included, are presented for nonstoichiometric $(\text{NaI})_n\text{Na}^+$ and $(\text{CsI})_n\text{Cs}^+$ ($n \leq 14$) cluster ions. The ground state and several low-lying isomers are identified and described. Rocksalt ground states are common and appear at cluster sizes lower than in the corresponding neutral systems. The most salient features of the measured mobilities seem to be explained by arguments related to the changes of the compactness of the clusters as a function of size. The stability of the cluster ions against evaporation of a single alkali halide molecule shows variations that explain the enhanced stabilities found experimentally for cluster sizes $n=4, 6, 9,$ and 13 . Finally, the ionization energies and the orbital eigenvalue spectrum of two $(\text{NaI})_{13}\text{Na}^+$ isomers are calculated and shown to be a fingerprint of the structure. [S0163-1829(98)03939-3]

I. INTRODUCTION

Alkali halide clusters have received substantial experimental and theoretical attention. From the experimental side, they are relatively easy to form, and their ionic bonding character has allowed the development of simple models for the interaction between the ions that form the cluster. They provide a nice opportunity to study the emergence of condensed-matter properties. An important point in this respect is the determination of the most stable isomers for each cluster size.

In this paper, we present the results of *ab initio* calculations of the structures and stabilities of $(\text{NaI})_n\text{Na}^+$ and $(\text{CsI})_n\text{Cs}^+$ clusters with $n=1-14$. Large clusters of these materials were first produced by bombardment of crystalline targets with Xe^+ ions and detected by means of secondary-ion mass spectrometry.¹⁻³ The mass spectra showed anomalies in the cluster intensities for certain values of n , which were tentatively interpreted as revealing the enhanced stability of ‘‘cuboidlike’’ structures. The results were explained in terms of a direct emission model, which assumes that cuboidlike cluster ions are directly sputtered from the crystal. Ens, Beavis, and Standing⁴ performed time-of-flight measurements for $(\text{CsI})_n\text{Cs}^+$ clusters, again produced by bombardment of CsI crystals, and considered different observation times after cluster emission. In that way, they found that the anomalies in the mass spectra were a consequence of evaporative decay *after* production of the cluster ions, and that the preferred decay channel was the ejection of a CsI molecule. Anomalies in the mass spectra of clusters formed by the inert-gas condensation technique were observed by Pflaum, Sattler and Recknagel.⁵ Twu *et al.* published mass spectra of sodium chloride, sodium iodide, cesium chloride, and cesium iodide cluster ions⁶ produced by laser vaporiza-

tion. They observed the same magic numbers for all those materials, namely, $n=4, 6, 9,$ and 13 in the small-size range. The differences in the detailed structure of the mass spectra were attributed to the relative sizes of the ions making up the clusters. All of those techniques, however, give no direct information regarding the cluster shapes. Drift cell experiments, which measure the mobility of the cluster ions and stand as a promising technique for structural analysis of clusters, have been performed to study the structures of small covalent and metallic clusters.⁷⁻¹⁰ More recently, ion mobility experiments have been performed for alkali halide clusters¹¹ and have revealed isomerization transitions^{12,13} in $(\text{NaCl})_n\text{Cl}^-$.

It was pointed out by Martin¹⁴ that precise measurements of the photoionization spectrum should also help in determining the structure of clusters of ionic materials. The reason is that, due to the strong localization of the electrons in closed-shell alkali halide clusters, the structure of the photoionization spectrum should be a fingerprint of the structure of the cluster, giving information on the set of inequivalent anions. Li and co-workers used this idea to correlate the optical absorption spectra of $(\text{CsI})_n\text{Cs}^+$ with the structures obtained by using a pair potential model.¹⁵⁻¹⁷ Photoelectron and photoionization spectroscopy as well as theoretical studies have also been performed to study the relation between the cluster structure and the localization mode for small alkali halide clusters with excess electrons,¹⁸⁻²¹ and to study the structure and emergence of metallic properties in alkali-rich alkali halide and alkali hydride clusters.²²⁻²⁶

Some theoretical calculations for alkali halide clusters have been based on phenomenological pair potential models.^{14,17,27-29} Such simplified models have been successful in explaining their main characteristics, and furthermore, are very useful for finding the different local minima in the

potential energy surface. *Ab initio* calculations performed by Ochsenfeld and co-workers^{30–32} used molecular orbital methods including correlation at the MP2 level. We have used the *ab initio* perturbed-ion (PI) model,³³ which is formulated within the restricted Hartree-Fock (RHF) approximation, in studies of neutral stoichiometric alkali halide^{34–36} and (MgO)_n clusters,³⁷ and in a preliminary study of non-stoichiometric (NaCl)_nNa⁺ clusters.³⁸ In some of those studies correlation contributions were included using an unrelaxed Coulomb-Hartree-Fock (uCHF) model proposed by Clementi.^{39,40} The PI model represents a major advance with respect to pair potential methods and provides an alternative description to the molecular orbital methods. In this paper we present an extensive study of charged (NaI)_nNa⁺ and (CsI)_nCs⁺ clusters with *n* up to 14. The results are aimed to assist in the interpretation of the experimental investigations of the structure of alkali halide clusters, as provided by the ion mobility studies, or of the relation between structure and photoionization spectrum.

The remainder of this paper is organized as follows: In Sec. II we briefly review the computational method used in this study. In Sec. III we report the results for the isomer structures, relative stabilities, and ionization potentials. Section IV summarizes our conclusions.

II. COMPUTATIONAL METHOD

The *ab initio* perturbed ion model,³³ as adapted to the study of ionic clusters, has been described at length in our previous work.^{34,35} In brief, the HF equations of the cluster are self-consistently solved in localized Fock spaces, by breaking the cluster wave function into local nearly orthogonal ionic wave functions and accounting for ion-cluster consistency. The average binding energy per ion of the (AX)_nA⁺ cluster is given by

$$E_{\text{bind}} = \frac{1}{2n+1} [nE_0(X^-) + (n+1)E_0(A^+) - E_{\text{cluster}}], \quad (1)$$

where $E_0(A^+)$ and $E_0(X^-)$ are the energies of the free cation A^+ and anion X^- , respectively. The localized nature of the PI model wave functions has some advantages. In weakly overlapping systems, the correlation energy is almost intra-atomic. In this paper, the correlation energy correction is obtained through Clementi's Coulomb-Hartree-Fock method.^{39,40} The PI model also allows for the development of efficient computational codes⁴¹ which make use of large multizeta Slater-type basis sets^{42,43} for the description of the ions. Our calculations have been performed using the following basis sets: (11s9p5d) for Cs⁺, taken from Ref. 43; (5s4p) for Na⁺, and (11s9p5d) for I⁻, both taken from Ref. 42. As input geometries for the optimization of the atomic structure we have considered the structures obtained from pair potential calculations.^{14,17,28,29} Those input geometries have been fully relaxed for (NaI)_nNa⁺ ($n \leq 6$) and (CsI)_nCs⁺ ($n \leq 4$) clusters, that is, the total cluster energy has been minimized with respect to variations in all the (3*N* - 6) independent coordinates, where *N* is the number of ions. For larger clusters, full relaxations are expensive and we have relaxed these structures with respect to a limited number of relevant parameters, which depend on the spatial

symmetry of each isomer. A downhill simplex algorithm has been used in all the optimizations.⁴⁴ All the cluster energies are converged within a precision of 1 meV.

III. RESULTS

A. Structures of isomers

The calculated structures of small (NaI)_nNa⁺ and (CsI)_nCs⁺ clusters are shown in Figs. 1 and 2, respectively. Small spheres represent cations and large spheres represent anions. The most stable structure, or ground state (GS) is shown on the left side for each cluster size. The other structures represent low-lying isomers. Below each isomer, the energy difference with respect to the ground state is given. The structures exhibit several distinct motives which can be roughly classified in chains, rocksalt pieces, and rings (mainly hexagonal). It is possible that other isomers could exist between the ground state and the low-lying isomers plotted in the figure, since our search has been limited mainly to the structures provided by pair potential calculations,^{14,17,28,29} and the possibility of overlooking some isomers cannot be excluded. For $n \geq 10$, the rocksalt motives consistently dominate the ground state and the crystalline structure emerges, although signs of the appearance of the rocksalt structure are also found for some of the clusters with $n < 10$. Let us describe first the structures obtained for the smaller cluster sizes. A linear chain is obtained as the ground state of (NaI)₂Na⁺. Bent chains, a rhombus with a cation attached, and a three-dimensional isomer are found to be less stable. All of those structures are closer in energy for (CsI)₂Cs⁺ and its three-dimensional GS is degenerate with the linear chain. The same GS structure is found for both materials at $n=3$, namely, a cube with an anion removed. The linear chain is still the second isomer for NaI, while it is found at a higher energy in CsI. A planar rocksalt piece plus a cation appears as a high-lying isomer. The rest of the isomers are obtained by attaching a molecule in several ways to some of the $n=2$ structures. The $n=4$ GS can be described as a quasi-two-dimensional sheet, which is quite curved in NaI but almost planar for CsI. The chain isomers are not competitive anymore. A cube with a cation attached is obtained as the second isomer. Again an essentially two-dimensional sheet, derived from the GS structure of (NaI)₄Na⁺ is the GS of (NaI)₅Na⁺. This isomer is still more stable than the three-dimensional (3D) structures, although the $2 \times 2 \times 3$ rocksalt piece with a corner anion removed is energetically very close. This notation indicates the number of ions along the *x*, *y*, and *z* directions, respectively. For CsI, a cube with a linear chain on top is obtained as the GS. The tendency for three-dimensional structures is stronger for the Cs clusters. Rounded cages with quadrangular and hexagonal faces form the GS for $n=6$ and $n=7$ in Fig. 1. Rocksalt isomers are still high in energy, although an hexagonal isomer is only 0.02 eV above the GS in (NaI)₆Na⁺. GS structures with higher coordination are obtained for CsI at these cluster sizes: a centered hexagonal prism for $n=6$, and a complex structure containing a cube for $n=7$. We can notice that the centered hexagonal prism is also related to the rocksalt structure since the central cation is coordinated to six ions. Both in the ground state and in the low-lying isomers discussed until now ($n \leq 7$) we appreciate a tendency to

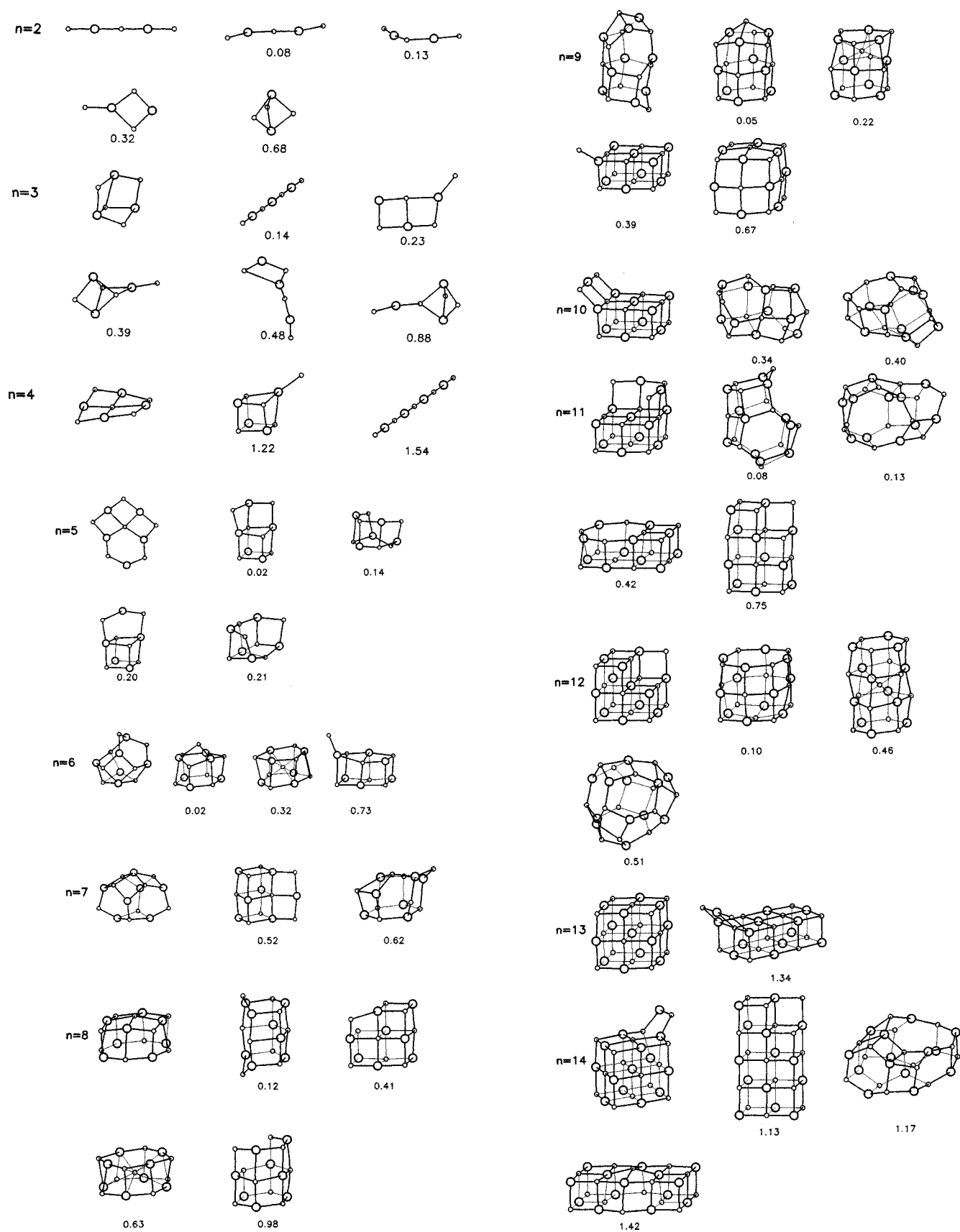


FIG. 1. Lowest-energy structure and low-lying isomers of $(\text{Na})_n\text{Na}^+$. The energy difference (in eV) with respect to the most stable structure is given below the corresponding isomers.

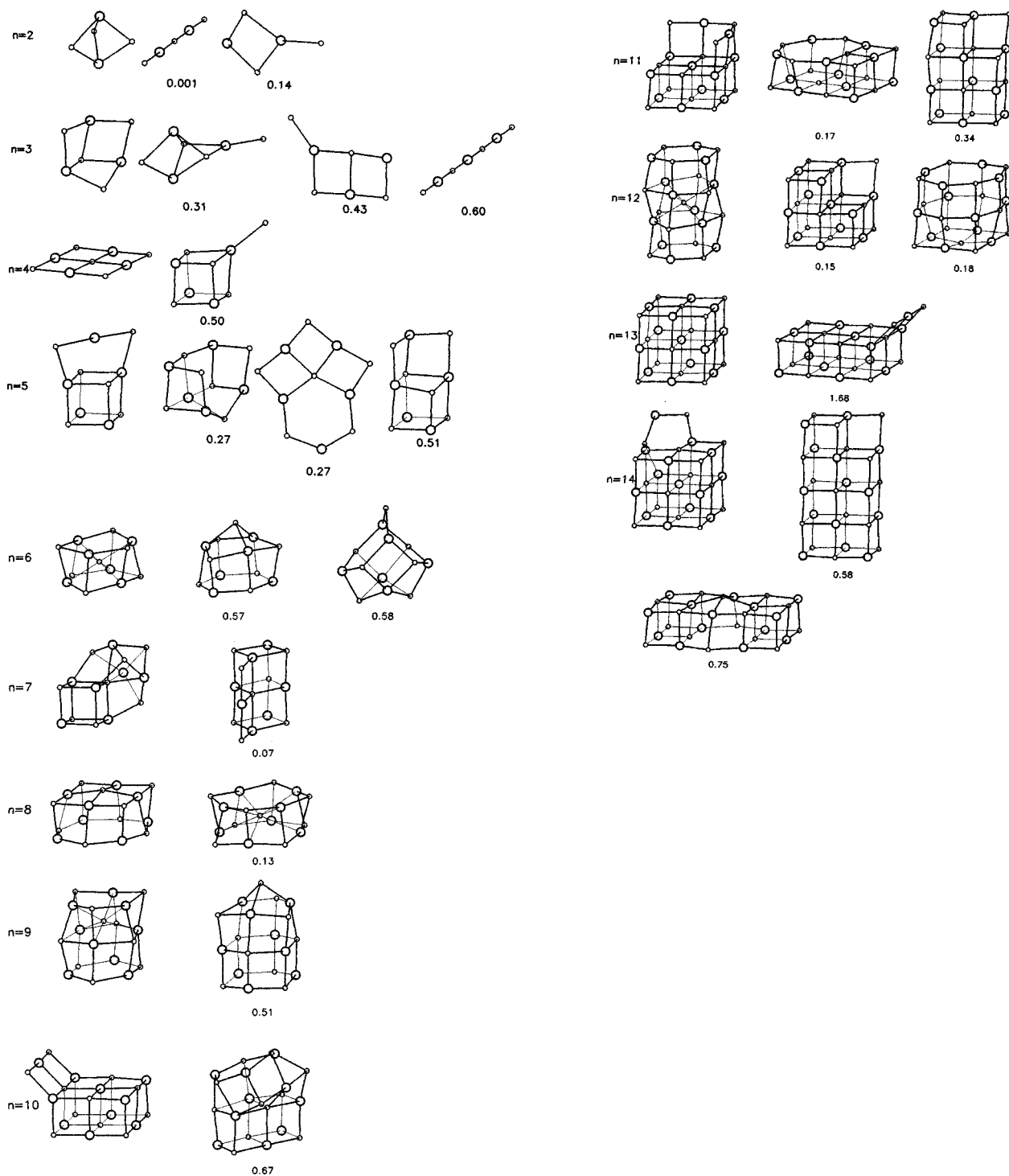


FIG. 2. Lowest-energy structure and low-lying isomers of $(\text{CsI})_n \text{Cs}^+$. The energy difference (in eV) with respect to the most stable structure is given below the corresponding isomers.

distorted structures that, in the more extreme cases leads to elongated clusters. This is driven by the excess positive charge. The distortion (elongation) lowers the repulsion between cations.

A $3 \times 3 \times 2$ -like structure with an anion missing from the center of a basal plane is obtained as the GS for $n=8$. The absence of this cation induces a distortion of that basis to an octagonal ring. A structure with an eight-coordinated cation is close to the GS for CsI. Eight is the coordination number of solid CsI. Structures obtained by adding a cation in sev-

eral ways to the hexagonal prismatic form of $(\text{NaI})_9$ (which is the GS of the neutral cluster³⁵) are the most stable $(\text{NaI})_9 \text{Na}^+$ isomers. In the GS, this cation induces a strong cluster deformation. The $(\text{CsI})_9 \text{Cs}^+$ GS is also related to an hexagonal prism. Cuboidlike rocksalt structures are less stable in both systems, but we can again notice that the upper half of the hexagonal prism is distorted in $(\text{CsI})_9 \text{Cs}^+$, and contains an inner cation with coordination six (the rocksalt coordination). Starting with $n=10$ the emergence of cuboidlike rocksalt features becomes apparent. From $n=10$ to n

=14, all the NaI GS clusters have the rocksalt structure. Notice, in particular, the high stability for $n=13$. More open structures with lower average coordination, or based on a stacking of rings, are less stable. The same can be said of CsI, with due exception of $n=12$, where a hexagonal prismatic structure (although with a central six-coordinated cation) is more stable.

The structural trends of neutral alkali halide clusters have been studied in Ref. 36. Those trends were rationalized in terms of the relative ion sizes. As the ratio r_C/r_A between the cation and anion radii increases, the tendency to form rocksalt fragments becomes enhanced. NaI has a small value of this ratio (0.44) while CsI has a large ratio (0.76). In spite of this difference, the charged nonstoichiometric clusters behave in a similar way. Rocksalt pieces appear early; about three quarters of the clusters between $n=3$ and $n=14$ have a rocksalt fragment, or a closely related structure, as the GS. The exceptions occur for $n=6,7,9$; in these cases the rocksalt isomers have one or two low-coordinated cations. One can notice the influence of nonstoichiometry and net charge: the percent of GS rocksalt structures in neutral $(\text{NaI})_n$ is only about one-half.³⁵ The reason seems to be that hexagonal prismatic structures are less competitive for the charged nonstoichiometric clusters. A perfect prism formed by hexagonal rings has an equal number of cations and anions, so only defect structures, obtained by removing an anion or by adding a cation, can be built for nonstoichiometric clusters. We find one example of the first type in one of the isomers of $(\text{NaI})_5\text{Na}^+$. A cation can be added on top of a terminal ring or in the interstitial hole between two hexagonal rings: isomers of both types exist for $(\text{NaI})_6\text{Na}^+$. These only become competitive when the rocksalt isomers are very unstable, as for $n=6,9$.

Pair potential calculations have been performed by Diefenbach and Martin²⁸ and Li and Whetten¹⁷ for these two systems. A comparison with the PI results shows some discrepancies. The pair potential calculations for $(\text{NaI})_n\text{Na}^+$ with $n=8, 10, 11, 12$, and 14 predict rather complex GS structures (independently of the use or not of polarization terms) which correspond to some of the isomers in Fig. 1, whereas the PI calculations lead to rocksalt-type structures. For $(\text{CsI})_n\text{Cs}^+$ the discrepancies are rather insignificant. In the PI model the binding energy of the cluster can be written³⁵ as a sum of classical and quantum interaction energies between the ions plus a term that accounts for the radial deformation of the electronic cloud of the free ions (in practice the anions) in response to the environment. These energy contributions contain quantum many electron terms that, in principle, describe the interatomic interactions better than the empirical potentials. There is also a second type of discrepancies between the PI and pair potential calculations, although much less significant. These occur when the rigid-ion and polarizable-ion model potentials disagree with each other and the PI model agrees with one of them. These cases are found for $(\text{NaI})_n\text{Na}^+$ with $n=2, 5$, and for $(\text{CsI})_n\text{Cs}^+$ with $n=2,7,8,11,12$. In those cases the PI model agrees sometimes with the rigid-ion model and sometimes with the polarizable-ion model, but the two isomers involved are generally close in energy, so the nonuniformity of the agreement can be ascribed to the small energy differences involved. In addition one has to bear in mind that, due to one basic as-

sumption of the PI model (spherically symmetric electron density clouds, centered on the nuclei), the polarization contribution coming from dipolar terms is absent in this model.

Kreisle and co-workers¹¹ have studied the mobility of $(\text{NaI})_n\text{Na}^+$ and $(\text{CsI})_n\text{Cs}^+$ clusters under the influence of an electric field in a chamber filled with helium gas. In these experiments the mobility is larger the lower the He scattering cross section by the cluster, and this cross section is inversely related to the compactness of the cluster. Kreisle and co-workers have plotted the inverse mobilities as a function of cluster size. Some salient features are common to the two curves and, in our opinion, can be related to the structural features found in Figs. 1 and 2. The main feature is a clear drop in the inverse mobility between $n=12$ and $n=13$. In fact, the inverse mobility becomes a local minimum for $(\text{NaI})_{13}\text{Na}^+$. It is suggestive to associate the high mobility of $n=13$ to its compact ‘‘perfect cube’’ form. Other feature is a visible change (decrease) of the slope of the inverse mobility curve at $n=4$. It is tentative to associate this to the change from the two-dimensional to more compact three-dimensional character of the ground state of $(\text{CsI})_n\text{Cs}^+$ between $n=4$ and $n=5$. Although the calculated GS of $(\text{NaI})_5\text{Na}^+$ is planar, there is a low-lying isomer, only 0.02 eV higher in energy, that could easily be present in the beam and contribute to increase the mobility.

B. Relative stabilities as a function of cluster size and comparison with experiment

The experimental mass spectra of alkali halide cluster ions¹⁻⁶ show intensity anomalies that reflect the special stability of some cluster sizes. In order to study the relative stability of $(\text{NaI})_n\text{Na}^+$ and $(\text{CsI})_n\text{Cs}^+$ cluster ions, we plot in Fig. 3 the average binding energies per ion [Eq. (1)] as a function of n . Maxima or pronounced changes of slope in these curves are considered as indicators of enhanced stability. Clear maxima at $n=4$ and $n=13$, and main slope changes at $n=6$ and $n=10$, are obtained for $(\text{NaI})_n\text{Na}^+$. For $(\text{CsI})_n\text{Cs}^+$ a maximum is apparent at $n=13$, and main slope changes occur at $n=4, 6$, and 9. Those features correlate with the observed abundance maxima. The most prominent observed maximum¹⁻⁶ is $n=13$. The magic numbers at $n=4, 6$, and 9, and specifically the enhanced abundances of $(\text{NaI})_6\text{Na}^+$ and $(\text{NaI})_9\text{Na}^+$ clusters,⁶ are less pronounced. The only discrepancy between experiment and theoretical predictions occurs for $(\text{NaI})_9\text{Na}^+$. However, the slope changes in Fig. 3 are so weak that the average binding energies are not the best indicators of the enhanced stability of some magic clusters.

The quantity E_{bind} measures the cluster stability with respect to the infinitely separated ions. The experiments indicate, however, that the abundance mass spectrum should be probably best explained in terms of the stability against evaporation of an alkali halide molecule.^{4,6,29} The energy required to remove a molecule AI from an $(AI)_nA^+$ cluster ion ($A=\text{Na,Cs}$) is given by

$$E_{evaporation} = E_{clus}[(AI)_{n-1}A^+] + E(AI) - E_{clus}[(AI)_nA^+] \quad (2)$$

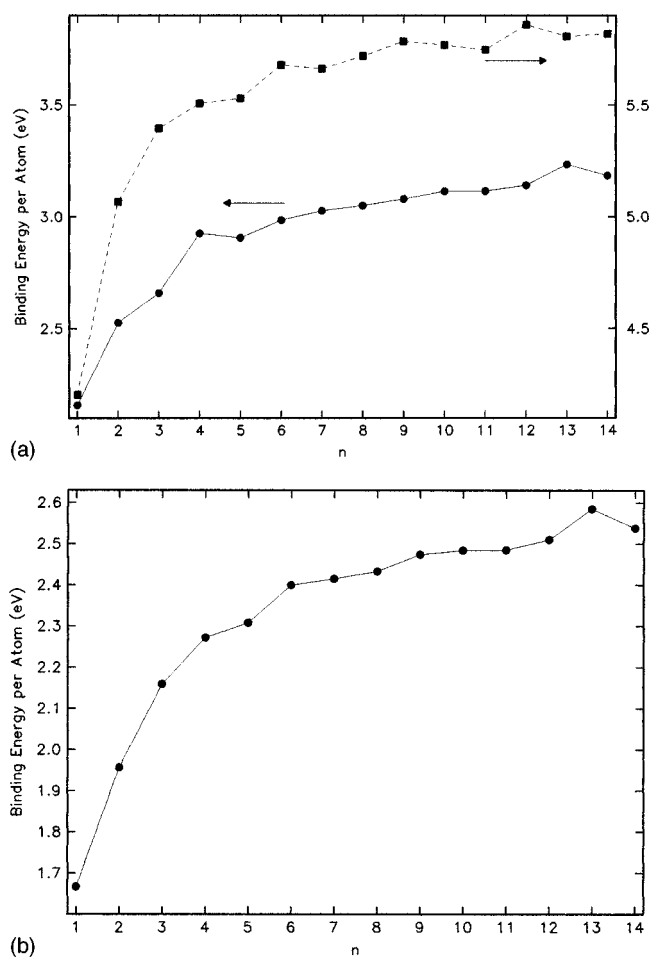


FIG. 3. Binding energy per ion as a function of the cluster size of $(\text{NaI})_n\text{Na}^+$ (circles) and $(\text{NaI})_n$ (squares) in (a) and of $(\text{CsI})_n\text{Cs}^+$ in (b).

The evaporation energies are plotted in Fig. 4. A sharp increase in the evaporation energy between $n=14$ and $n=13$, between $n=10$ and $n=9$, between $n=7$ and $n=6$, and finally between $n=5$ and $n=4$ is evident for the $(\text{CsI})_n\text{Cs}^+$ clusters. This means that evaporative cooling will result in enrichment of clusters with $n=4, 6, 9$, and 13 in the beam. The results are similar for $(\text{NaI})_n\text{Na}^+$, predicting enrichment of clusters with $n=4, 6$, and 13 , but a discrepancy with respect to experiment is again obtained since enrichment is predicted for $n=10$, instead of $n=9$. In an attempt to resolve this discrepancy we have also plotted in Fig. 4 a “vertical” evaporation energy. This is defined by removing from the parent cluster (size n) the least-bound molecule (this can be identified in the PI model, since the total binding energy of the cluster can be separated into a sum of ion contributions; see Refs. 33–36 for details), and relaxing the resulting structure (size $n-1$) to its nearest local minimum. This is in many cases not the ground state of the $(n-1)$ cluster and the difference between the “adiabatic” and “vertical” evaporation energies in Fig. 4 accounts for this fact. In spite of this difference the use of vertical evaporation energies leads to the same predictions for $(\text{CsI})_n\text{Cs}^+$ as before, but changes the predictions for $(\text{NaI})_n\text{Na}^+$ to improve agreement with experiment for $n=9$, which is a maximum in the curve of the

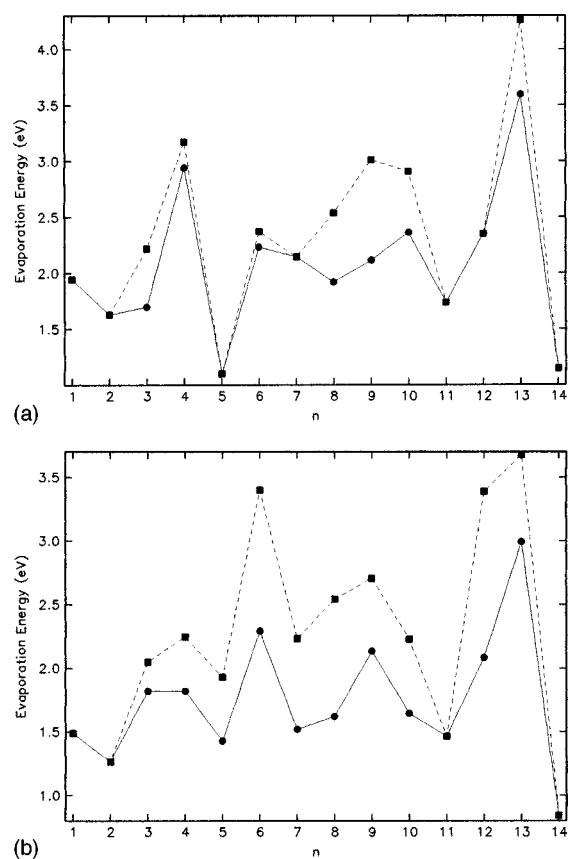


FIG. 4. Adiabatic (circles) and vertical (squares) energies required to evaporate a neutral molecule from $(\text{NaI})_n\text{Na}^+$ (a) and $(\text{CsI})_n\text{Cs}^+$ (b) clusters as a function of n .

vertical evaporation energies. The interpretation is that, although the adiabatic evaporation of a molecule from $(\text{NaI})_{10}\text{Na}^+$ costs more energy than adiabatic evaporation from $(\text{NaI})_9\text{Na}^+$, there are in both cases isomeric forms of the $(n-1)$ clusters with (i) a structure similar to that of the n cluster and (ii) large energy barriers between those isomeric forms and the ground state structure of the $(n-1)$ cluster, such that the vertical evaporation from $(\text{NaI})_9\text{Na}^+$ is larger. In summary, our calculations suggest the possible relevance of isomers of the $(n-1)$ cluster with a structure similar to that of the GS of the n cluster to explain the details of the mass spectra when evaporative cooling is involved. This point deserves further investigation. The main magic numbers $n=4$ and $n=13$ are a consequence of the enhanced stability of very symmetrical rocksalt structures, in two and three dimensions, respectively. On the other hand, $n=6$ and $n=9$ are “fine-structure” peaks of the spectra and the explanation in terms of structural features is less evident. These occur for $(\text{CsI})_n\text{Cs}^+$ because structures are formed that optimize the value of the Madelung energy more efficiently than for neighboring cluster sizes. $(\text{CsI})_9\text{Cs}^+$ has some highly coordinated ions: one cation with coordination 6 and three anions with coordination 5. $(\text{CsI})_6\text{Cs}^+$ also contains one cation with coordination 6. At the same time the lowest coordination found in these two clusters is 3. In contrast, some of the neighbor clusters, such as $(\text{CsI})_5\text{Cs}^+$ and $(\text{CsI})_{10}\text{Cs}^+$, contain some ions with coordination 2. Those-

highly coordinated structures are less competitive for $(\text{NaI})_6\text{Na}^+$ and $(\text{NaI})_9\text{Na}^+$. Figure 3(a) also shows, for comparison, the binding energies per ion of neutral stoichiometric $(\text{NaI})_n$ clusters.³⁵ The local maxima occur for $n=6$, 9, and 12, and have been associated with the formation of compact structures with large atomic coordination compared to clusters with $n+1$ and $n-1$ molecules.

C. Ionization energies and structure

In previous studies of alkali-halide clusters,^{34,35} we have analyzed the variation of the ionization potential (IP) with the cluster size. The vertical IP was calculated in the Koopmans' approximation as the binding energy of the lowest bound electron in the cluster, which is of course located on a specific anion. Here we investigate the relation between the geometrical structure and the spectrum of electronic states for different isomers of the same cluster. This could provide a way to distinguish isomers, already explored for other types of clusters.⁴⁵ In the PI model the electrons near the highest occupied molecular orbital level are localized on distinct anions, and the different eigenvalues arise from the different atomic environment around nonequivalent anions. Thus, the set of one-electron energy eigenvalues characteristic of each isomer can be considered as a fingerprint of its structural shape.¹⁴ As an example, we present in Fig. 5 the orbital energy spectrum corresponding to the two isomers of $(\text{NaI})_{13}\text{Na}^+$ given in Fig. 1. It is apparent that the two isomers have quite different spectra. These could be measured by photoelectron spectroscopy, and, in principle, it could be possible to determine the structure of the different isomers present in a mass-selected beam by comparing the experimental spectra with theoretical results. In our example, only two peaks are expected in the lowest-energy part of the spectrum for the case of the GS isomer, because the symmetry of this structure induces high degeneracies. One of the peaks corresponds to removing one electron from any of the twelve surface anions (labeled A in the figure) and is identified with the vertical IP. The other corresponds to the removal of one electron from the central anion (labeled B) with coordination 6. The second isomer has a larger number of inequivalent anions and the spectrum is broader. Besides, the ionization energy is 1.3 eV lower than for the GS isomer. Similar "fingerprints" distinguish different isomers for other cluster sizes.

IV. SUMMARY

The determination of the structures of alkali halide cluster isomers is a challenging subject for present-day experimental techniques.^{11,12} Theoretical calculations can throw light on these problems. In this paper, we present *ab initio* calculations of the structures and stabilities of $(\text{NaI})_n\text{Na}^+$ and $(\text{CsI})_n\text{Cs}^+$ cluster ions with $n \leq 14$. Starting from several local minima found with phenomenological pair potential models, we have used the perturbed-ion model (with correlation included) in order to determine the ground state and some low-lying isomers. Our results indicate an early formation of rocksalt fragments. The rocksalt features appear at values of n lower than in the corresponding neutral species.^{35,36} Arguments related to the compactness of some clusters appear to be able to explain the main features ob-

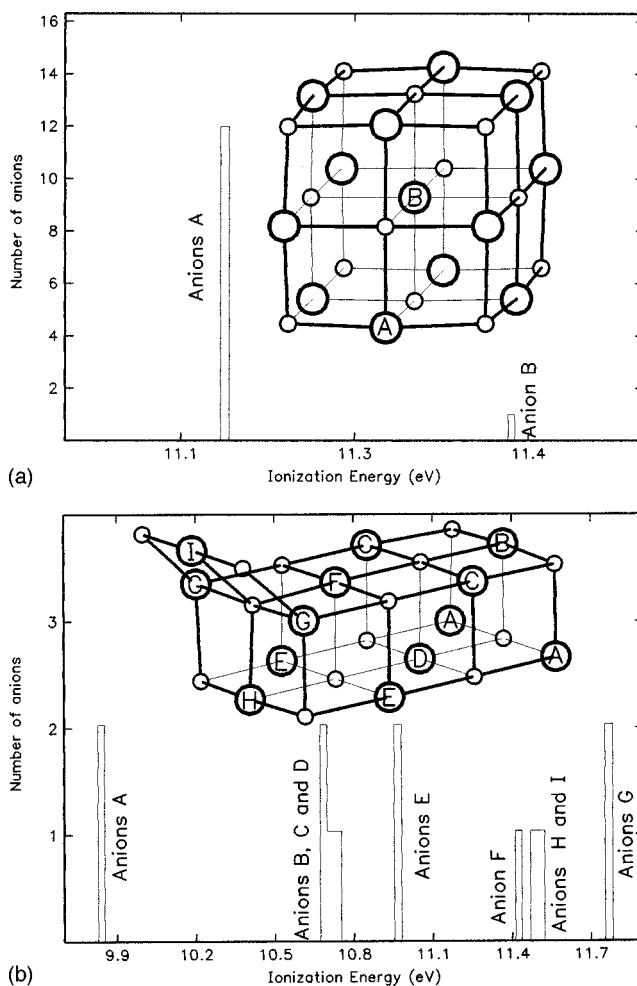


FIG. 5. Spectrum of orbital energy eigenvalues for the two isomers of $(\text{NaI})_{13}\text{Na}^+$ studied. Inequivalent anions are labeled with different letters. The vertical scale gives the number of equivalent anions of each type.

tained in the mobility measurements of Kreisle and co-workers.¹¹ The mass spectra obtained by several experimental techniques¹⁻⁶ show evidence of enhanced population for cluster sizes $n=4, 6, 9$, and 13. Our calculations confirm the enhanced stability of these clusters, namely, those clusters are very stable against evaporation of a single molecule. We have investigated the possibility to determine isomeric structures by comparing experimental photoelectron spectra with those obtained theoretically. As an example we have shown how the spectra of orbital energy eigenvalues of two $(\text{NaI})_{13}\text{Na}^+$ isomers depend on the structure. With all these results in mind, we are confident that the identification of the isomer structures of clusters of ionic materials, may be feasible in the near future if experimental and theoretical efforts work together.

ACKNOWLEDGMENTS

This work was supported by DGES (PB95-0720-CD2-01) and Junta de Castilla y León (VA63/96). A. Aguado was supported by Junta de Castilla y León. A. Ayuela acknowledges support by the EU TMR program.

- ¹T. M. Barlak, J. E. Campana, R. J. Colton, J. J. DeCorpo, and J. R. Wyatt, *J. Phys. Chem.* **85**, 3840 (1981).
- ²J. E. Campana, T. M. Barlak, R. J. Colton, J. J. DeCorpo, J. R. Wyatt, and B. I. Dunlap, *Phys. Rev. Lett.* **47**, 1046 (1981).
- ³T. M. Barlak, J. R. Wyatt, R. J. Colton, J. J. DeCorpo, and J. E. Campana, *J. Am. Chem. Soc.* **104**, 1212 (1982).
- ⁴W. Ens, R. Beavis, and K. G. Standing, *Phys. Rev. Lett.* **50**, 27 (1983).
- ⁵R. Pflaum, K. Sattler, and E. Recknagel, *Phys. Rev. B* **33**, 1522 (1986).
- ⁶Y. J. Twu, C. W. S. Conover, Y. A. Yang, and L. A. Bloomfield, *Phys. Rev. B* **42**, 5306 (1990).
- ⁷G. von Helden, Y. T. Hsu, P. R. Kemper, and M. T. Bowers, *J. Chem. Phys.* **95**, 3835 (1991).
- ⁸D. E. Clemmer, K. B. Shelimov, and M. F. Jarrold, *Science* **260**, 784 (1993).
- ⁹J. M. Hunter, J. L. Fye, E. J. Roskamp, and M. F. Jarrold, *J. Phys. Chem.* **98**, 1810 (1994).
- ¹⁰M. F. Jarrold, *J. Phys. Chem.* **99**, 11 (1995).
- ¹¹M. Maier-Borst, P. Löffler, J. Petry, and D. Kreisle, *Z. Phys. D* **40**, 476 (1997).
- ¹²R. R. Hudgins, P. Dugourd, J. M. Tenenbaum, and M. F. Jarrold, *Phys. Rev. Lett.* **78**, 4213 (1997).
- ¹³J. P. K. Doye and D. J. Wales, cond-mat/9801152 (unpublished).
- ¹⁴T. P. Martin, *Phys. Rep.* **95**, 167 (1983).
- ¹⁵X. Li, R. D. Beck, and R. L. Whetten, *Phys. Rev. Lett.* **68**, 3420 (1992).
- ¹⁶X. Li and R. L. Whetten, *Z. Phys. D* **26**, 198 (1993).
- ¹⁷X. Li and R. L. Whetten, *J. Chem. Phys.* **98**, 6170 (1993).
- ¹⁸Y. A. Yang, L. A. Bloomfield, C. Jin, L. S. Wang, and R. E. Smalley, *J. Chem. Phys.* **96**, 2453 (1992).
- ¹⁹G. Durand, F. Spiegelmann, P. Labastie, J.-M. L'Hermite, and Ph. Poncharal, *Phys. Rev. Lett.* **79**, 633 (1997); U. Landman, R. N. Barnett, C. L. Cleveland, and G. Rajagopal, in *Physics and Chemistry of Finite Systems: From Clusters to Crystals*, edited by P. Jena, S. N. Khanna, and B. K. Rao (Kluwer, Dordrecht, 1992), Vol. 1, p. 165.
- ²⁰D. J. Fatemi, F. K. Fatemi, and L. A. Bloomfield, *Phys. Rev. A* **54**, 3674 (1996).
- ²¹F. K. Fatemi, D. J. Fatemi, and L. A. Bloomfield, *Phys. Rev. Lett.* **77**, 4895 (1996).
- ²²N. Yu, P. Xia, L. A. Bloomfield, and M. Fowler, *J. Chem. Phys.* **102**, 4965 (1995).
- ²³V. Bonacić-Koutecký, J. Pittner, and J. Koutecký, *Chem. Phys.* **210**, 313 (1996), and references therein; R. N. Barnett, H. P. Cheng, H. Hakkinen, and U. Landman, *J. Phys. Chem.* **99**, 7731 (1995).
- ²⁴R. Antoine, Ph. Dugourd, D. Rayane, E. Benichou, and M. Broyer, *J. Chem. Phys.* **107**, 2664 (1997).
- ²⁵D. J. Fatemi, F. K. Fatemi, and L. A. Bloomfield, *Phys. Rev. B* **55**, 10 094 (1997).
- ²⁶S. Frank, N. Malinowski, F. Tast, M. Heinebrodt, I. M. L. Billas, and T. P. Martin, *J. Chem. Phys.* **106**, 6217 (1997).
- ²⁷D. O. Welch, O. W. Lazareth, G. J. Dienes, and R. D. Hatcher, *J. Chem. Phys.* **64**, 835 (1976).
- ²⁸J. Diefenbach and T. P. Martin, *J. Chem. Phys.* **83**, 4585 (1985).
- ²⁹N. G. Phillips, C. W. S. Conover, and L. A. Bloomfield, *J. Chem. Phys.* **94**, 4980 (1991).
- ³⁰C. Ochsenfeld and R. Ahlrichs, *J. Chem. Phys.* **101**, 5977 (1994).
- ³¹C. Ochsenfeld, J. Gauss, and R. Ahlrichs, *J. Chem. Phys.* **103**, 7401 (1995).
- ³²C. Ochsenfeld and R. Ahlrichs, *Ber. Bunsenges. Phys. Chem.* **99**, 1191 (1995).
- ³³V. Luaña and L. Pueyo, *Phys. Rev. B* **41**, 3800 (1990).
- ³⁴A. Ayuela, J. M. López, J. A. Alonso, and V. Luaña, *Z. Phys. D* **26**, S213 (1993); *An. Fis.* **90**, 190 (1994); *Physica B* **212**, 329 (1996).
- ³⁵A. Aguado, A. Ayuela, J. M. López, and J. A. Alonso, *J. Phys. Chem.* **101B**, 5944 (1997).
- ³⁶A. Aguado, A. Ayuela, J. M. López, and J. A. Alonso, *Phys. Rev. B* **56**, 15 353 (1997).
- ³⁷E. de la Puente, A. Aguado, A. Ayuela, and J. M. López, *Phys. Rev. B* **56**, 7607 (1997).
- ³⁸A. Ayuela, J. M. López, J. A. Alonso, and V. Luaña, *Can. J. Phys.* **76**, 311 (1998).
- ³⁹E. Clementi, *IBM J. Res. Dev.* **9**, 2 (1965).
- ⁴⁰S. J. Chakravorty and E. Clementi, *Phys. Rev. A* **39**, 2290 (1989).
- ⁴¹V. Luaña, A. Martín Pendás, J. M. Recio, and E. Francisco, *Comput. Phys. Commun.* **77**, 107 (1993).
- ⁴²E. Clementi and C. Roetti, *At. Data Nucl. Data Tables* **14**, 177 (1974).
- ⁴³A. D. McLean and R. S. McLean, *At. Data Nucl. Data Tables* **26**, 197 (1981).
- ⁴⁴W. H. Press and S. A. Teukolsky, *Comput. Phys.* **5**, 426 (1991).
- ⁴⁵N. Bingelli and J. R. Chelikowsky, *Phys. Rev. Lett.* **75**, 493 (1995).